Lacoste, E., **Fréour, S.,** Jacquemin, F. (2010). On the validity of the Kröner-Eshelby scale transition model for inclusions with various morphologies, *Mechanics of Materials*, **42**(2), 218-226.

On the validity of the Kröner-Eshelby scale transition model for inclusions with varying morphologies

E. Lacoste, F. Jacquemin, S. Fréour

Institut de Recherche en Génie Civil et Mécanique (UMR CNRS 6183),

Université de Nantes – Centrale Nantes, 37 Boulevard de l'Université,

BP 406, 44 602 Saint-Nazaire cedex, France

Abstract

Scale transition models based on Eshelby's solution provide interesting information on the properties and multi-scale mechanical states experienced by materials presenting complex microstructures, such as composite materials, accounting for the constituents' properties but also microstructural parameters such as the morphology of the heterogeneous inclusions constituting the material. Nevertheless, these approaches cannot reliably account for multiple inclusion morphologies in the same representative elementary volume of the modeled material, predicting two distinct sets of properties depending of the quantities (strains or stresses) used to formulate the homogenization procedure.

The present work aims to investigate the validity of Eshelby-Kröner self-consistent model in the case when several morphologies do coexist within the same representative elementary volume. A study of the two available formulations and their limits leads to suggest a mixed formulation inspired of Vook-Witt's model, which satisfies Hill's averages principles. The results of this formulation are also described in the case of a thermo-mechanical solicitation.

KeyWords

Kröner – Eshelby self-consistent model, multiple inclusions, random orientation, multiscale behaviour, composite materials.

1 INTRODUCTION

The recent development of composite materials during the last two decades opened new prospectives to mechanical part engineering, particularly for aeronautical applications, because of their high strength-to-weight ration as well as corrosion and fatigue resistance. But, as a counterpart of these advantages, the inherent heterogeneity of these material induce complex mechanical behaviours under service solicitations, and also internal stresses produced during the cure and tooling processes of a part.

Thus, the need for predicting the stress repartition among the constituents gave a boost to the development of the so-called "scale transition models", which permit to relate the behaviours of the material at several scales of interest. Among these, Eshelby-Kröner self-consistent model ([Kocks and al., 1998]) or Eshelby's solution based models (like Mori-Tanaka estimates) suggest a realistic and interesting approach, which enables to calculate the homogenized properties of the material, and also to predict the stress repartition between the constituents. The first applications concerned polycrystals, possibly multi-phased, this topic still being of current interest ([François, 1991], [Fréour, 2003]). These models are also interesting for composite materials, owing to the high heterogeneity of their constituents. Thereby, several recent papers have shown the relevance of these approaches for describing the hygro-mechanical and thermo-mechanical behaviour of composite structures ([Fréour and al., 2006], [Fréour and al., 2005], [Jacquemin and al., 2005]).

These models have been applied to new industrial materials that present a microstructure containing inclusions of various morphologies or geometrical orientations ([Baptiste, 2003], [Le Pen and Baptiste, 2002]). This kind of microstructure also corresponds to nano-composites, constituted of very rigid and stretched (about 50nm-long and 5nm-wide) carbon nanotubes with random geometrical orientation, embedded in a low-stiffness organic matrix. Nanotubes are still used at a very low volume content (below 1%), but show extremely interesting mechanical properties and notably a Young's modulus higher than 1TPa ([Treacy and al., 1996]), which promises very important future developments.

Eshelby's solution-based homogenization procedures can be formulated from both of Hill's averages principles (see relation [3] and [4] below), which link local and macroscopic behaviours through strains and stresses, respectively. Actually, when all the BVs ??? have the same morphology, both conditions are satisfied and the two formulations are equivalent. Nevertheless, [Benveniste, 1987] has shown that this was not the case, a priori, when the inclusions constituting the material presented several morphologies. In this case, the strain-based and stress-based formulations lead to distinct effective properties, verifying Hill's averages principles for stresses **or** strains, but never simultaneously both of them.

In a first part, the classical scale transition formalism set up by Hill and Eshelby is extended to the case when materials present a complex morphological microstructure (i.e., when the uniqueness of the BV morphology is not satisfied). The formulations based on the volume averages over stresses and strains are described within the framework of a Kröner-Eshelby model with multiple morphologies, leading to two sets of relations for the effective properties. In a second part, the model is used to describe the multiscale behaviour of a composite material with a random distribution of the geometrical orientation of the reinforcing strips. A double scale transition homogenization procedure is developed and applied to the material; the results for effective properties and respect of Hill's averages principles are discussed for the two formulations. A mixed formulation is then suggested and confirmed.
In the last part, this formulation is used to predict local stresses in the material subjected to mechanical and thermal loadings.

2 GENERAL PRESENTATION OF THE MULTIMORPHOUS MODEL

2.1 Hill's formalism and Kröner-Eshelby model

Kröner-Eshelby scale transition model is based on a representation of the material at several scales: on one hand, the « local » scale denoted by the superscript ^{i}, where we observe the behaviour of each constituent, considered as an ellipsoidal and homogeneous inclusion (also called Base Volume) ; on the other hand, the macroscopic scale denoted by the superscript ^{I}, where we can observe the behaviour of the Homogeneous Equivalent Medium (or HEM). These behaviours are expressed by the following thermo-elastic laws:

$$\boldsymbol{\sigma}^{\mathbf{I}} = \mathbf{L}^{\mathbf{I}} : \left(\boldsymbol{\varepsilon}^{\mathbf{I}} - \boldsymbol{\alpha}^{\mathbf{I}} \Delta \mathrm{T}\right) \qquad [1]$$

Lacoste, E., **Fréour, S.,** Jacquemin, F. (2010). On the validity of the Kröner-Eshelby scale transition model for inclusions with various morphologies, *Mechanics of Materials*, **42**(2), 218-226.

$$\boldsymbol{\sigma}^{\mathbf{i}} = \mathbf{L}^{\mathbf{i}} : \left(\boldsymbol{\varepsilon}^{\mathbf{i}} - \boldsymbol{\alpha}^{\mathbf{i}} \Delta \mathrm{T}\right) \qquad [2]$$

In these relations, the stiffnesses are represented by the 4th-order tensor **L**, and the Coefficients of Thermal Expansion (CTE) by the 2nd-order tensor $\boldsymbol{\alpha}$. The temperature increment is denoted by ΔT, whereas $\boldsymbol{\sigma}$ and $\boldsymbol{\varepsilon}$ stand for the stress and strain, respectively.

The scale transition relations are basically written as volume averages operations on stresses and strains. [Hill, 1967] showed, in a very general way, the equivalence between set (i.e. volume) averages and volume integrals. Hill's volume average relations over the mechanical states (also called consistency principles on mechanical states) are written:

$$\boldsymbol{\varepsilon}^{\mathbf{I}} = \left\langle \boldsymbol{\varepsilon}^{\mathbf{i}} \right\rangle \qquad [3]$$

$$\boldsymbol{\sigma}^{\mathbf{I}} = \left\langle \boldsymbol{\sigma}^{\mathbf{i}} \right\rangle \qquad [4]$$

where the square brackets $\langle ... \rangle$ represent the arithmetical volume average.

In a fundamental work, Eshelby studied the behavior of an inclusion embedded in an homogeneous medium loaded at the infinite [Eshelby, 1957]. He demonstrated that, if and only if the inclusion had an ellipsoidal shape, the local stresses and strains where homogeneous inside the BV, and fulfilled the following relation:

$$\boldsymbol{\sigma}^{\mathrm{i}} - \boldsymbol{\sigma}^{\mathrm{I}} = -\mathbf{L}^{\mathbf{I}} : \mathbf{R}^{\mathbf{I}} : \left(\boldsymbol{\varepsilon}^{\mathrm{i}} - \boldsymbol{\varepsilon}^{\mathrm{I}}\right) \qquad [5]$$

where $\mathbf{R}^{\mathbf{I}}$ is the adimensionnal reaction tensor, which represents the interaction between the inclusion and its surrounding medium.
The Kröner-Eshelby and Mori-Tanaka models both use this relation, considering the constituents as Eshelby inclusions. For the Kröner-Eshelby model, the embedding medium is given the properties of the HEM. As a consequence, the expressions giving the effective properties are implicit and require iterative solving methods, which only give numerical solutions. However, this approach accounts for every interaction between the particles ??? and leads to much more reliable local mechanical states, in comparison with more simple approaches as Mori-Tanaka's ([Berryman and Berge, 1996]).

The reaction tensor $\mathbf{R}^{\mathbf{I}}$ can be written from the Eshelby tensor $\mathbf{S}^{\mathbf{I}}_{\mathbf{esh}}$ or the Morris tensor $\mathbf{E}^{\mathbf{I}}$, thanks to the following relation (where **I** is the 4th-order Identity tensor):

$$\mathbf{R}^{\mathbf{I}} = \left(\mathbf{I} - \mathbf{S}^{\mathbf{I}}_{\mathbf{esh}}\right) : {\mathbf{S}^{\mathbf{I}}_{\mathbf{esh}}}^{-1} = \left({\mathbf{L}^{\mathbf{I}}}^{-1} - \mathbf{E}^{\mathbf{I}}\right) : {\mathbf{E}^{\mathbf{I}}}^{-1} \qquad [6]$$

The Morris tensor expresses the interaction of an inclusion with a given morphology (independently of its elastic properties) and the HEM; it has the dimension of a compliance tensor. In the case of an ellipsoidal inclusion whose principal axes lengths are $\{2a_1, 2a_2, 2a_3\}$, it is written in the coordinate system of the inclusion:

$$\mathbf{E}^{\mathbf{I}}_{\mathbf{ijkl}} = \frac{1}{4\pi} \int_0^{\pi} \sin\theta . d\theta \int_0^{2\pi} \boldsymbol{\gamma}^{\mathbf{I}}_{\mathbf{ijkl}} . d\varphi \text{ with } \boldsymbol{\gamma}^{\mathbf{I}}_{\mathbf{ijkl}} = \left(\mathbf{K}^{\mathbf{I}}_{\mathbf{ik}}\right)^{-1} . \xi_j . \xi_l \qquad \mathbf{[7]}$$

Lacoste, E., **Fréour, S.,** Jacquemin, F. (2010). On the validity of the Kröner-Eshelby scale transition model for inclusions with various morphologies, *Mechanics of Materials*, **42**(2), 218-226.

In the case of an orthotropic macroscopic symmetry, the $K_{ik}(\xi)$ components are given in the reference [Kröner, 1953]:

$$\mathbf{K^I} = \begin{bmatrix} L^I_{11}\,\xi_1{}^2 + L^I_{66}\,\xi_2{}^2 + L^I_{55}\,\xi_3{}^2 & \left(L^I_{12}+L^I_{66}\right)\xi_1\,\xi_2 & \left(L^I_{13}+L^I_{55}\right)\xi_1\,\xi_2 \\ \left(L^I_{12}+L^I_{66}\right)\xi_1\,\xi_2 & L^I_{66}\,\xi_1{}^2 + L^I_{22}\,\xi_2{}^2 + L^I_{44}\,\xi_3{}^2 & \left(L^I_{23}+L^I_{44}\right)\xi_2\,\xi_3 \\ \left(L^I_{13}+L^I_{55}\right)\xi_1\,\xi_2 & \left(L^I_{23}+L^I_{44}\right)\xi_2\,\xi_3 & L^I_{55}\,\xi_1{}^2 + L^I_{44}\,\xi_2{}^2 + L^I_{33}\,\xi_3{}^2 \end{bmatrix}$$

where $\xi_1 = \dfrac{\sin\theta\cos\varphi}{a_1}$, $\xi_2 = \dfrac{\sin\theta\sin\varphi}{a_2}$, $\xi_3 = \dfrac{\cos\theta}{a_3}$.

Some computations of the Morris tensor are given in [Kocks and al., 1998 ; Mura, 1982], who also give a detailed presentation of the Kröner-Eshelby model. Because of the complex expression of the integrand $\boldsymbol{\gamma}^{\mathbf{I}}_{\mathbf{ijkl}}$, one cannot generally give an analytical expression of $\mathbf{E^I}$, except for some specific configurations (fibers, discs and spheres in particular). The calculation of this tensor is thereby a key-point of the models based on Eshelby's inclusion.
Furthermore, specific attention must be paid to the fact that the calculation of the Morris tensor must be made on the stiffness tensor $\mathbf{L^I}$ dropped in the coordinate system Ri of the inclusion. In the lack of an isotropy with respect to the rotation carried out, several new non-null components appear in $\mathbf{L^I}$, thus invalidating the expression of $\mathbf{K^I}$ given by Kröner for more convenient situations.

If the inclusions constituting the material do not present a single morphology in the macroscopic coordinate system RI, the tensors $\mathbf{R^I}, \mathbf{S^I_{esh}}$ and $\mathbf{E^I}$ are not purely macroscopic anymore but related to the considered BV also; in consequence, the superscript $^{\mathbf{I}}$ will be replaced by $^{\mathbf{Ii}}$. The transition between the local and macroscopic coordinate systems is made through the convention introduced in [Roe, 1965]. In order to lighten the equations, the tensors will be implicitly dropped in RI for the averaging operations.

2.2 Formulation with stresses and strains

Starting form the local and macroscopic behaviour laws, and using the scale transition relation given above (Equation [7]), one can express the local stresses and strains as:

$$_{\mathbf{Ri}}\boldsymbol{\varepsilon}^{\mathbf{i}} = {}_{\mathbf{Ri}}\left(\mathbf{L^i} + \mathbf{L^I} : \mathbf{R^{Ii}}\right)^{-1} : \left[{}_{\mathbf{Ri}}\left(\mathbf{L^I} + \mathbf{L^I} : \mathbf{R^{Ii}}\right) : {}_{\mathbf{Ri}}\boldsymbol{\varepsilon}^{\mathbf{I}} + {}_{\mathbf{Ri}}\left(\mathbf{L^I} : \boldsymbol{\alpha}^{\mathbf{I}} - \mathbf{L^i} : \boldsymbol{\alpha}^{\mathbf{i}}\right)\Delta T\right] \qquad [8]$$

$$_{\mathbf{Ri}}\boldsymbol{\sigma}^{\mathbf{i}} = {}_{\mathbf{Ri}}\mathbf{L^i} : {}_{\mathbf{Ri}}\left(\mathbf{L^i} + \mathbf{L^I} : \mathbf{R^{Ii}}\right)^{-1} : \left[{}_{\mathbf{Ri}}\left(\mathbf{L^I} + \mathbf{L^I} : \mathbf{R^{Ii}}\right) {}_{\mathbf{Ri}}\mathbf{L^{I}}^{-1} : {}_{\mathbf{Ri}}\boldsymbol{\sigma}^{\mathbf{I}} + {}_{\mathbf{Ri}}\mathbf{L^I} :_{\mathbf{Ri}} \mathbf{R^{Ii}} :_{\mathbf{Ri}} \left(\boldsymbol{\alpha}^{\mathbf{I}} - \boldsymbol{\alpha}^{\mathbf{i}}\right)\Delta T\right] \qquad [9]$$

One would notice that the term $_{\mathbf{Ri}}\left(\mathbf{L^i} + \mathbf{L^I} : \mathbf{R^{Ii}}\right)^{-1} :_{\mathbf{Ri}} \left(\mathbf{L^I} + \mathbf{L^I} : \mathbf{R^{Ii}}\right)$ which appears in the equation [8] is equivalent to the elastic strain localization tensor: $_{\mathbf{Ri}}\mathbf{A^i_i} = \left[{}_{\mathbf{Ri}}\mathbf{E^{Ii}} : ({}_{\mathbf{Ri}}\mathbf{L^i} - {}_{\mathbf{Ri}}\mathbf{L^I}) + \mathbf{I}\right]^{-1}$. The same is true for the elastic stress concentration tensor: $\mathbf{B^i} = \mathbf{L^i} : \mathbf{A^i} : \mathbf{L^{I}}^{-1}$ that appears in the expression of the local stresses. These tensors are defined, for elastic solicitations, by the two relations:

$$\boldsymbol{\varepsilon}^{\mathbf{i}} = \mathbf{A^i} : \boldsymbol{\varepsilon}^{\mathbf{I}} \qquad [10]$$

$$\boldsymbol{\sigma}^{\mathbf{i}} = \mathbf{B^i} : \boldsymbol{\sigma}^{\mathbf{I}} \qquad [11]$$

Of course, Hill's averages principles imply the following relation on $\mathbf{A^i}$ and $\mathbf{B^i}$:

$$\left\langle \mathbf{A^i} \right\rangle = \left\langle \mathbf{B^i} \right\rangle = \mathbf{I} \qquad [12]$$

Hill's averages principles can be written on both strains and stresses; nevertheless, only one relation is needed to obtain the effective properties, which leads to two alternate expressions. Thus, if using Hill's average principle on stress, one would write the macroscopic stress as:

$$\begin{aligned} \boldsymbol{\sigma}^{\mathbf{I}} &= \left\langle \mathbf{L^i} : \left(\mathbf{L^i} + \mathbf{L^I} : \mathbf{R^{Ii}}\right)^{-1} : \left(\mathbf{L^I} + \mathbf{L^I} : \mathbf{R^{Ii}}\right) : \mathbf{L^I}^{-1} \right\rangle : \boldsymbol{\sigma}^{\mathbf{I}} \\ &+ \left\langle \mathbf{L^i} : \left(\mathbf{L^i} + \mathbf{L^I} : \mathbf{R^{Ii}}\right)^{-1} : \mathbf{L^I} : \mathbf{R^{Ii}} : \left(\boldsymbol{\alpha}^{\mathbf{I}} - \boldsymbol{\alpha}^{\mathbf{i}}\right) \right\rangle \Delta \mathrm{T} \end{aligned} \qquad [13]$$

The relation being satisfied for any macroscopic state $\{\boldsymbol{\sigma}^{\mathbf{I}}, \Delta\mathrm{T}\}$, one obtains:

$$\left\langle \mathbf{L^i} : \left(\mathbf{L^i} + \mathbf{L^I} : \mathbf{R^{Ii}}\right)^{-1} : \left(\mathbf{L^I} + \mathbf{L^I} : \mathbf{R^{Ii}}\right) : \mathbf{L^I}^{-1} \right\rangle = \left\langle \mathbf{L^i} : \mathbf{A^i} : \mathbf{L^I}^{-1} \right\rangle = \left\langle \mathbf{B^i} \right\rangle = \mathbf{I} \qquad [14]$$

$$\left\langle \mathbf{L^i} : \left(\mathbf{L^i} + \mathbf{L^I} : \mathbf{R^{Ii}}\right)^{-1} : \mathbf{L^I} : \mathbf{R^{Ii}} : \left(\boldsymbol{\alpha}^{\mathbf{I}} - \boldsymbol{\alpha}^{\mathbf{i}}\right) \right\rangle = \mathbf{0} \qquad [15]$$

The relation [14] implies the following expression for the effective stiffness:

$$\mathbf{L^I} = \left\langle \mathbf{L^i} : \mathbf{A^i} \right\rangle \qquad [16]$$

In a same way, a few algebric manipulations of the relation [15] give an expression of the effective CTE:

$$\boldsymbol{\alpha}^{\mathbf{I}} = \left\langle \mathbf{L^i} : \left(\mathbf{L^i} + \mathbf{L^I} : \mathbf{R^{Ii}}\right)^{-1} : \mathbf{L^I} : \mathbf{R^{Ii}} \right\rangle^{-1} : \left\langle \mathbf{L^i} : \left(\mathbf{L^i} + \mathbf{L^I} : \mathbf{R^{Ii}}\right)^{-1} : \mathbf{L^I} : \mathbf{R^{Ii}} : \boldsymbol{\alpha}^{\mathbf{i}} \right\rangle \qquad [17]$$

On the contrary, if one uses Hill's average principle on strain, one would obtain:

$$\boldsymbol{\varepsilon}^{\mathbf{I}} = \left\langle \left(\mathbf{L^i} + \mathbf{L^I} : \mathbf{R^{Ii}}\right)^{-1} : \left[\left(\mathbf{L^I} + \mathbf{L^I} : \mathbf{R^{Ii}}\right) : \boldsymbol{\varepsilon}^{\mathbf{I}} + \left(\mathbf{L^I} : \boldsymbol{\alpha}^{\mathbf{I}} - \mathbf{L^i} : \boldsymbol{\alpha}^{\mathbf{i}}\right) \Delta \mathrm{T}\right] \right\rangle \qquad [18]$$

which implies the two following relations on elastic and thermal strains:

$$\left\langle \left(\mathbf{L^i} + \mathbf{L^I} : \mathbf{R^{Ii}}\right)^{-1} : \left(\mathbf{L^I} + \mathbf{L^I} : \mathbf{R^{Ii}}\right) \right\rangle = \left\langle \mathbf{A^i} \right\rangle = \mathbf{I} \qquad [19]$$

$$\left\langle \left(\mathbf{L^i} + \mathbf{L^I} : \mathbf{R^{Ii}}\right)^{-1} : \left(\mathbf{L^I} : \boldsymbol{\alpha}^{\mathbf{I}} - \mathbf{L^i} : \boldsymbol{\alpha}^{\mathbf{i}}\right) \right\rangle = \mathbf{0} \qquad [20]$$

One would then obtain the following effective properties:

Lacoste, E., **Fréour, S.,** Jacquemin, F. (2010). On the validity of the Kröner-Eshelby scale transition model for inclusions with various morphologies, *Mechanics of Materials*, **42**(2), 218-226.

$$\mathbf{L^I} = \mathbf{L^I} : \left\langle \mathbf{A^i} \right\rangle = \left\langle \mathbf{L^{i}}^{-1} : \mathbf{B^i} \right\rangle^{-1} \qquad [21]$$

$$\boldsymbol{\alpha}^{\mathbf{I}} = \mathbf{L^I}^{-1} : \left\langle \left(\mathbf{L^i} + \mathbf{L^I} : \mathbf{R^{Ii}} \right)^{-1} \right\rangle^{-1} : \left\langle \left(\mathbf{L^i} + \mathbf{L^I} : \mathbf{R^{Ii}} \right)^{-1} : \mathbf{L^i} : \boldsymbol{\alpha}^{\mathbf{i}} \right\rangle \qquad [22]$$

Several authors have shown that, if the inclusions had a unique morphology in the macroscopic coordinate system, the two formulations led to a same set of effective properties. That's why the model is widely used for metals [Fréour, 2003] (with spherical inclusions), and for unidirectional composite plies with organic [Fréour and al., 2006] or metallic matrix [Le Pen and Baptiste, 2002]. On the other hand, in the case that the material exhibits a morphological texture with a distribution of the inclusion geometry, one obtains two solutions that satisfy Hill's average principle on strains or stresses, but never both of them. [Benveniste, 1987] noticed this drawback of the Eshelby-based models, but no systematic study of it can be found in the bibliography. That's why we will study and compare the results given by each formulation, for a composite material with planar isotropy.

3 APPLICATION TO AN IN-PLANE ISOTROPIC MATERIAL

We focus on a high-performance composite material developed for the design of composite parts to be used for aeronautical applications. This material is made of unidirectional reinforcing strips with rectangular shape (60x8x0.15 mm) and randomly disposed in the layout (see Figure 2). The strips themselves are composed of T300 fibers and epoxy matrix, set as a unidirectional ply. The material then appears as a thick layout (1.3mm) with in-plane isotropy. The properties of the epoxy resin and the T300 fibers are given in [Jacquemin and al., 2005] and [Agbossou, 1997]; they are summed up in the Table 1 below.

3.1 Description of the scale transition procedure

The Kröner-Eshelby model is used in order to perform a two-steps scale transition (see Figure 1): First, the effective properties of the reinforcing strip are estimated from those of the intra-reinforcements matrix and the carbon fibers. Then, a homogenization procedure is achieved in order to find the behaviour of the material ~~is homogenized~~, from the properties of the extra-reinforcements matrix and those of the reinforcing strips (previously estimated).

Figure 1 : Schematic representation of the two steps scale transition

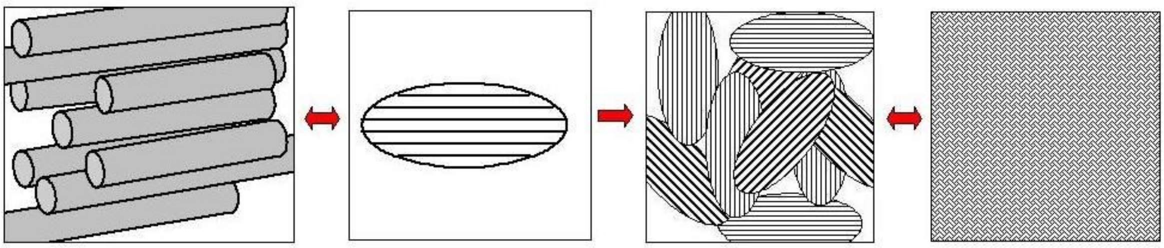

The homogenization of the reinforcing strip is not a particular matter as it corresponds to the case, treated in a recent paper ([Jacquemin and al., 2005]), of an unidirectionally reinforced composite ply. Consequently, one will only give the effective properties of the reinforcing strip (see Table 1), accounting for a fiber volume ration of 63%.

Table 1: Thermomechanical properties of a reinforcing strip (estimated by the Kröner-Eshelby model), and its constituents

	Mechanical moduli						CTE		Density
	E_x (GPa)	E_y, E_z (GPa)	ν_{xy}, ν_{xz}	G_{xy}, G_{xz} (GPa)	ν_{yz}	G_{yz} (GPa)	α_x (10^{-6}/K)	α_y, α_z (10^{-6}/K)	ρ (kg/m^3)
Reinforcing strips	146.8	10.2	0.274	7.0	0.355	3.8	-0.620	48.0	1620
T300 fibers	230	15	0.20	15	0.07	7	-1.5	27	1866.67
N5208 matrix	4.5	4.5	0.4	1.61	0.4	1.61	60	60	1200

On the other hand, the second scale transition involves stretched and non-oriented inclusions and thus depends upon the multimorphous model, as described in the next sections.
In order to lighten the expressions, a "local" coordinate system R_{xyz}, oriented along the axis of the fibers constituting the strips, is introduced. This coordinate is obtained by a rotation Θ around the 3-axis of the "global" coordinate system R_{123} bound to the effective material.

Figure 2: Schematic representation of the microstructure of the material

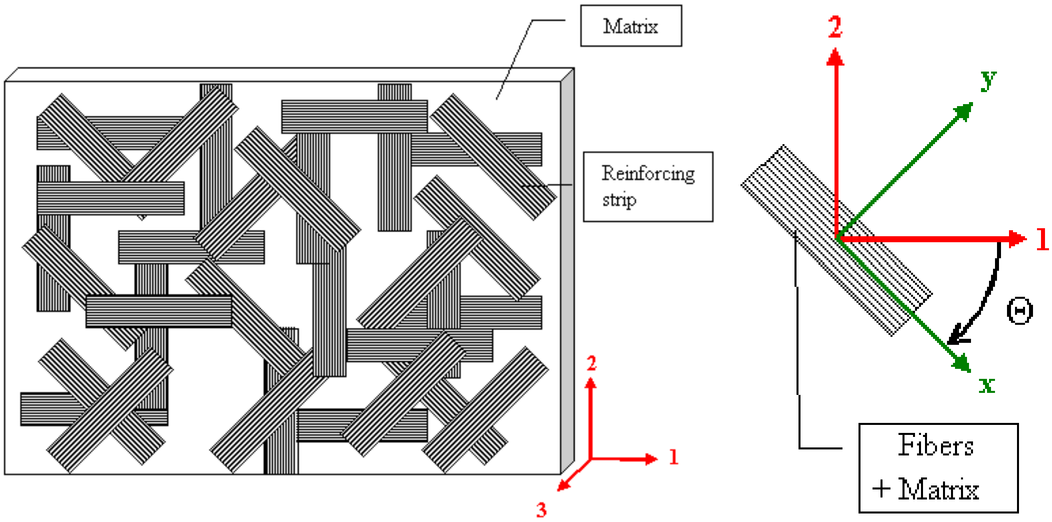

3.2 Effective properties of the material for each formulation

The equations [16] and [21] provide the effective stiffness of the material with 10^{-3} accuracy, for both formulations. The averaging operations are achieved onto the two previously described constituents (reinforcing strips with 95% volume ratio and extra-reinforcement matrix with 5% ratio). A set of 10 orientations uniformly distributed on 180° in the 1-2 plan is considered in order to account for the morphology texture. The effective elastic moduli obtained are summed up in the Table 2.
These moduli verify, within the prescribed accuracy, the Reuss and Voigt bounds (see Table 2). The elastic moduli obtained according to the homogenization procedure satisfying Hill's average principle over strains are close to the Reuss bound; whereas those obtained by the approach satisfying Hill's average principle over stresses are practically merged with the Voigt bound.
Furthermore, the two methods lead to drastically different stiffnesses, particularly for the components that govern the in-plane behaviour (E_1, ν_{12} and G_{12}). On the contrary, the "out-of-plane" components (E_3, ν_{13} and G_{13}) do not vary very much from an homogenization procedure to another.

Lacoste, E., **Fréour, S.,** Jacquemin, F. (2010). On the validity of the Kröner-Eshelby scale transition model for inclusions with various morphologies, *Mechanics of Materials*, **42**(2), 218-226.

Table 2: Elastic moduli of the material (isotropic in the 1-2 plan), estimated by the Kröner-Eshelby model, for the two formulations

	E_1, E_2 (GPa)	E_3 (GPa)	ν_{12}	G_{12} (GPa)	ν_{13}, ν_{23}	G_{13}, G_{23} (GPa)
Hε	16.63	9.92	0.121	7.42	0.337	4.45
Hσ	55.48	11.24	0.290	21.49	0.266	3.97
Voigt bound	55.46	11.28	X	21.49	X	5.20
Reuss bound	15.44	9.66	X	6.65	X	4.46

Remark: The notations Hσ and Hε are used, respectively, to denote the stress-based and strain-based formulations.

Also, the computation of the averages for localization~~s~~ and concentration~~s~~ tensors, upon the two phases and all the orientations, show that none of the two methods respect both Hill's averages relations [3] and [4]. Actually, according to Table 3, equation [16] satisfies [4] but not [3], whereas equation [21] ensures that [3] is satisfied, but not [4] anymore. The error is concentrated on the "in-plane traction-compression" components ($A_{11} = A_{22}$), on "in-plane shear" (A_{66}) and mainly on out-of-plane components ($A_{44} = A_{55}$ and $A_{31} = A_{32}$). Nevertheless, we notice that these errors keep relatively low for the chosen morphology, in the order of 3% if the out-of-plane shear components are not considered.

On the contrary, for the homogenization with strains, the principle of means is insured for strains but not stresses (see Table 3). The errors are particularly significant for the in-plane components (250% relative error on $B_{11} = B_{22}$ and 60% absolute error on $B_{12} = B_{21}$), for the in-plane shear (190% error on B_{66}), as well as out-of-plane transverse components (120% error on $B_{13} = B_{23}$). On the other hand, the error is null for the out-of-plane components of compression-traction (B_{33}) and shear ($B_{44} = B_{55}$).

For both formulations, the in-plane components ($_{11}$, $_{12}$ and $_{66}$ components) exhibit very important errors over Hill's averages principles. For them, the stress-based formulation gives the lower errors; on the contrary, for the out-of-plane components, the strain-based formulation is the most reliable. One can also notice that the in-plane moduli E_1, ν_{12} and G_{12} are the most dependent of the formulation used. Comparatively, the out-of-plane moduli E_3, ν_{13} and G_{13} are relatively identical whatever the formulation used.

Table 3: Averages of the localization and concentration tensors for the in-plane isotropic material, homogenized with stresses or strains

$\langle A^i \rangle$	$A_{11} = A_{22}$	A_{33}	$A_{44} = A_{55}$	A_{66}	A_{12}	A_{21}	$A_{13} = A_{23}$	$A_{31} = A_{32}$
Hε	1.001	1	0.5	0.5	0	0	0	0
Hσ	1.031	1	0.443	0.512	0.007	0.007	0	-0.033
$\langle B^i \rangle$	$B_{11} = B_{22}$	B_{33}	$B_{44} = B_{55}$	B_{66}	B_{12}	B_{21}	$B_{13} = B_{23}$	$B_{31} = B_{32}$
Hε	3.465	1	0.5	1.431	0.604	0.604	-1.178	0
Hσ	1	1	0.5	0.5	0	0	0	0
Expected value	1	1	1/2	1/2	0	0	0	0

As above, the Coefficients of Thermal Expansion have been computed with respect to the two homogenization approaches previously presented in section 2.2. The thermal homogenization respecting Hill's average relations expressed over the strains is achieved owing to relation [22], using the effective stiffness obtained by relation [21]; respectively, the stress-based homogenization is done using the relation [17] and the effective stiffness obtained with relation [16]. This leads to the results presented in the Table 4 below. As for the stiffness, a significant deviation between the results occurs, depending on the homogenization procedure used. By the way, this discrepancy also exists in the case that the same stiffness is used for the two formulations.

Table 4: CTEs of the in-plane isotropic material, estimated by the Kröner-Eshelby model, for the two formulations, and associated errors

	CTE		Error on ε		Error on σ	
	α_1 , α_2 (10^{-6}/K)	α_3 (10^{-6}/K)	$\mathbf{X}_1^{\text{thermo}}$	$\mathbf{X}_3^{\text{thermo}}$	$\mathbf{Y}_1^{\text{thermo}}$	$\mathbf{Y}_3^{\text{thermo}}$
Hε	24.8	49.9	0	0	-2.088	0
Hσ	3.52	114.9	0.062	-0.424	0	0
Expected value	~4	~60	0	0	0	0

In order to quantify the relevance of these results, the adimensionnal errors $\mathbf{X}^{\text{thermo}}$ and $\mathbf{Y}^{\text{thermo}}$ are defined as follows:

$$\begin{cases} \mathbf{X}^{\text{thermo}} = \left\langle \Delta\boldsymbol{\varepsilon}^{\text{thermo},\mathbf{i}} \right\rangle : \left(\boldsymbol{\alpha}^{\mathbf{I}}\Delta \mathrm{T}\right)^{-1} \\ \mathbf{Y}^{\text{thermo}} = \left\langle \Delta\boldsymbol{\sigma}^{\text{thermo},\mathbf{i}} \right\rangle : \left(\mathbf{L}^{\mathbf{I}} : \boldsymbol{\alpha}^{\mathbf{I}}\Delta \mathrm{T}\right)^{-1} \end{cases} \quad [23]$$

where
$$\begin{cases} \Delta\boldsymbol{\sigma}^{\text{thermo},\mathbf{i}} = \mathbf{L}^{\mathbf{i}} : \left(\mathbf{L}^{\mathbf{i}} + \mathbf{L}^{\mathbf{I}} : \mathbf{R}^{\mathbf{I}}\right)^{-1} : \mathbf{L}^{\mathbf{I}} : \mathbf{R}^{\mathbf{I}} : \left(\boldsymbol{\alpha}^{\mathbf{I}} - \boldsymbol{\alpha}^{\mathbf{i}}\right)\Delta \mathrm{T} \\ \Delta\boldsymbol{\varepsilon}^{\text{thermo},\mathbf{i}} = \left(\mathbf{L}^{\mathbf{i}} + \mathbf{L}^{\mathbf{I}} : \mathbf{R}^{\mathbf{I}}\right)^{-1} : \left(\mathbf{L}^{\mathbf{I}} : \boldsymbol{\alpha}^{\mathbf{I}} - \mathbf{L}^{\mathbf{i}} : \boldsymbol{\alpha}^{\mathbf{i}}\right)\Delta \mathrm{T} \end{cases} \quad [24]$$

These errors are also presented in Table 4, for both formulations. One can thus observe that the strain-based formulation verifies Hill's averages principle over strains, but leads to some errors on thermal stresses and mainly in the normal direction. Respectively, the stress-based formulation verifies Hill's averages principle over stresses but underestimates the in-plane thermal strains by more than 200%.

Furthermore, some tests were made to study the evolution of the properties with the morphology of the reinforcing strips. We could observe that the two formulations merge when the inclusions have a circular (or penny-shaped) morphology, thus confirming the validity of the model for a unique morphology. Nevertheless, the gap between the two solutions, as well as the associated errors, quickly grows up as the morphology is stretched and thick.

3.3 Mixed formulation and results

From the study carried out in the previous section, one would conclude that none of the two discussed homogenization procedures can give ~~perfectly~~ satisfying results for the overall thermo-mechanical behaviour. But one can also point out that each one has a "preferential direction" where exhibited errors are low: thus, the stress-based formulation gives a satisfying description of the in-plane behaviour, while the strain-based formulation is well adapted to the out-of-plane behaviour.

The microstructure presented by the studied materials corresponds to an assembly of thin in-plane layers. Previous works achieved on similar structures suggested that extreme direction-dependent homogenization procedures such as the Vook-Witt model (see [Vook and Witt, 1968] and [Welzel and Freour, 2007]) gave satisfying results on both in-plane and out-of-plane behaviour. A mixed homogenenization is thereby suggested, where the in-plane behaviour is modeled using the stress-based formulation, whereas the strain-based formulation is used for the out-of-plane behaviour.

With this mixed formulation, the stiffness tensor of the material satisfies the following from:

$$\mathbf{L^I} = \begin{bmatrix} {}^{H\sigma}L^{I}_{11} & {}^{H\sigma}L^{I}_{12} & {}^{H\varepsilon}L^{I}_{13} & & & \\ {}^{H\sigma}L^{I}_{12} & {}^{H\sigma}L^{I}_{22} & {}^{H\varepsilon}L^{I}_{23} & & & \\ {}^{H\varepsilon}L^{I}_{31} & {}^{H\varepsilon}L^{I}_{32} & {}^{H\varepsilon}L^{I}_{33} & & & \\ & & & {}^{H\varepsilon}L^{I}_{44} & & \\ & & & & {}^{H\varepsilon}L^{I}_{44} & \\ & & & & & {}^{H\sigma}L^{I}_{66} \end{bmatrix} \qquad [25]$$

By injecting this expression in the computation loop of the stiffness, one obtains the results summed up in Table 5. One finds effective moduli very close to those obtained with the stress-based formulation (see Table 2), exception made of the G_{13} coefficient which is closer to the modulus homogenized with strains. We notice very little evolution of these elastic moduli if we (moderately) modify the shape ratios defining the morphology.

Table 5: Elastic moduli of the in-plane isotropic material, with the mixed formulation

E_1, E_2 (GPa)	E_3 (GPa)	ν_{12}	G_{12} (GPa)	ν_{13}, ν_{23}	G_{13}, G_{23} (GPa)
55.41	11.20	0.289	21.49	0.279	4.496

Furthermore, the computation of the averages of the localization and concentration tensors (Table 6) shows that Hill's averages principles are relatively well verified. The main errors are committed on the in-plane strains, for compression-traction (3% error on A_{11}) or shear strains (2% error on A_{66}). These errors grow up with the stretching and the thickness of the reinforcing strips, but are lower than those obtained with "pure" formulations.

Table 6: Averages of the localization and concentration tensors for the in-plane isotropic material, with the mixed formulation

$\langle \mathbf{A}^{\mathbf{i}} \rangle$	$A_{11} = A_{22}$	A_{33}	$A_{44} = A_{55}$	A_{66}	A_{12}	A_{21}	$A_{13} = A_{23}$	$A_{31} = A_{32}$
	1.029	1.000	0.500	0.511	0.007	0.007	0.000	-0.015
$\langle \mathbf{B}^{\mathbf{i}} \rangle$	$B_{11} = B_{22}$	B_{33}	$B_{44} = B_{55}$	B_{66}	B_{12}	B_{21}	$B_{13} = B_{23}$	$B_{31} = B_{32}$
	1.001	1.001	0.497	0.500	0.001	0.001	-0.009	0.001
Expected value	1	1	1/2	1/2	0	0	0	0

The same method is used for computing the effective CTE, which satisfies the following symmetry:

$$\boldsymbol{\alpha}^{\mathbf{I}} = \begin{bmatrix} {}^{H\sigma}\alpha^{I}_{11} & & \\ & {}^{H\sigma}\alpha^{I}_{11} & \\ & & {}^{H\varepsilon}\alpha^{I}_{33} \end{bmatrix} \qquad [26]$$

Lacoste, E., **Fréour, S.,** Jacquemin, F. (2010). On the validity of the Kröner-Eshelby scale transition model for inclusions with various morphologies, *Mechanics of Materials*, **42**(2), 218-226.

The resulting CTE are given in Table 7, which also sums up the errors on thermal stresses and strains, for the studied morphology (60x8x0.15). The mixed formulation provides good results in the considered case, with an error below 3% on thermal strains. By the way, this error becomes null for a penny-shaped morphology ($a_1 = a_2$).

Table 7: CTE of the in-plane isotropic material estimated by the Kröner-Eshelby model, for the mixed formulation, and associated errors

	CTE		Error on ε		Error on σ	
	α_1 , α_2 (10^{-6}/K)	α_3 (10^{-6}/K)	X_1^{thermo}	X_3^{thermo}	Y_1^{thermo}	Y_3^{thermo}
Hmixed	3.52	64.3	0.031	0.027	0.004	0.002
Expected value	~4	~60	0	0	0	0

4 APPLICATION TO THERMO-MECHANICAL LOADS

The proposed scale transition procedure enables to compute effective properties closed to experimental results; furthermore, it has been shown that the procedure enabled to estimate local stresses and strains consistent with the macroscopic solicitations. In this last section, this procedure will be used in order to predict the internal stresses in the material when subjected to mechanical and thermal loads.

4.1 Response of the material to purely mechanical load

In order to describe the multi-scale mechanical behaviour of the material, a macroscopic traction, in the 1-direction, of 100 MPa is considered. The relation [9] is used to compute the local strains in the constituents, dropped in the local coordinate system Ri. The stresses into the reinforcing strips and the extra-reinforcements matrix are first computed (Figure 3); from that result, the stresses into the constituents of the reinforcing strip (matrix and fibers) are also calculated (Figure 4).

One can observe that compression-traction stresses $\{\sigma_{xx}, \sigma_{yy}, \sigma_{zz}\}$ evolve as π-periodic cosinusoids, while shear stresses σ_{xy} evolve as sinusoids. These evolutions with orientation match the ones observed for composite laminates subjected to compression-traction loads. Inside the in-plane isotropic material (see Figure 3 below), the in-plane stresses are strongly heterogeneous (contrarily to the in-plane strains, which are rather almost homogeneous): the reinforcing strips experience up to 260 MPa in the x-direction, while the organic matrix undergoes less than 10 MPa. On the contrary, out-of-plane stresses are rather homogeneous and very low.

Figure 3: Local stresses in the material, depending on the orientation angle Θ

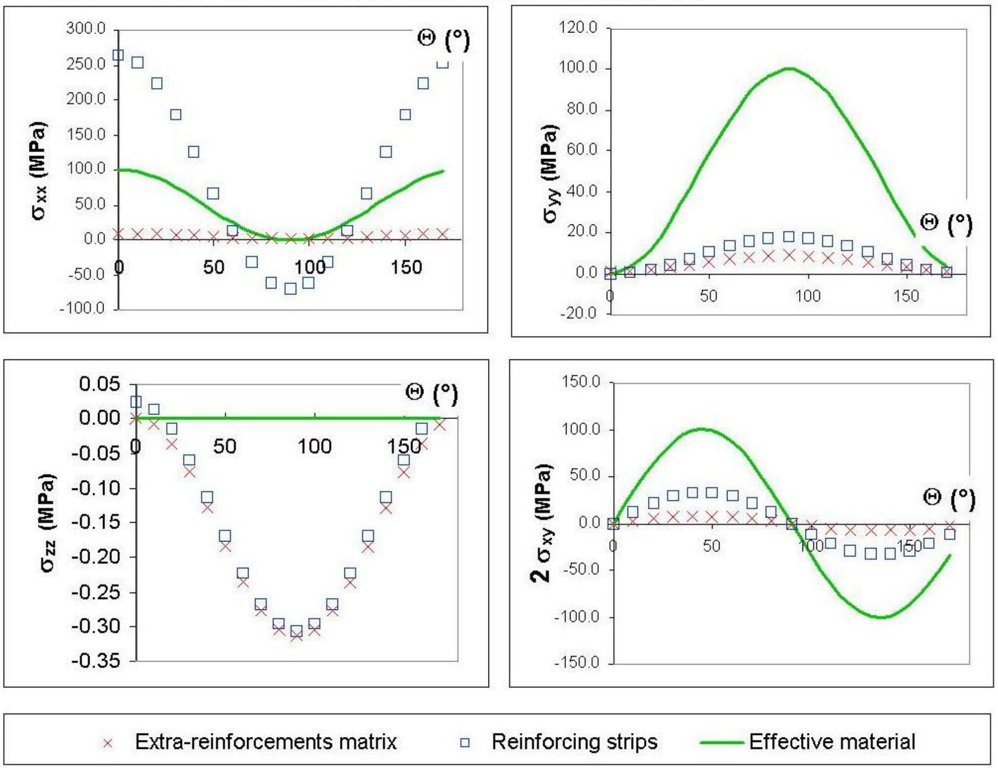

Figure 4: Local stresses in the reinforcing strip, depending on the orientation angle Θ

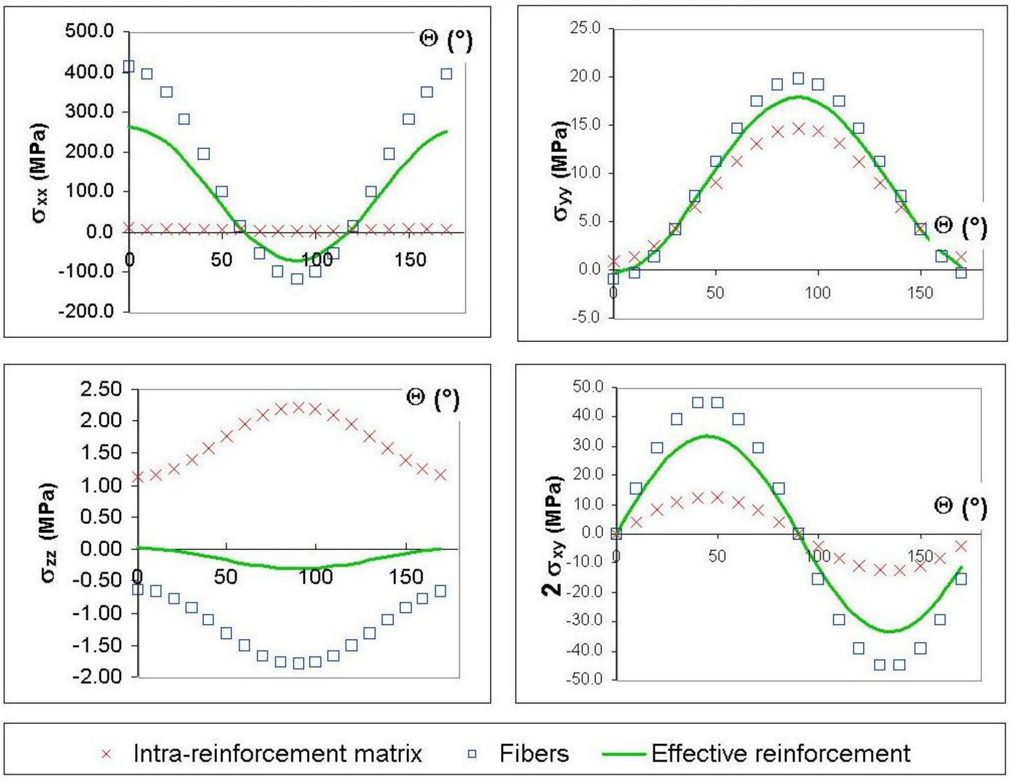

For the reinforcing strips (see Figure 4 above), one can observe a concentration of stresses in the fibers, particularly along the fiber-axis (where the strains are very homogeneous). The matrix takes very few stresses in the x-direction, and less than 20 MPa in the others directions. The out-of-plane stresses stay very low (-2 to 2.5 MPa) in comparison with in-plane stresses.

4.2 Response of the material to purely thermal load

A similar study was achieved for the in-plane isotropic material submitted to a -100°C thermal load. This kind of solicitation is typical of the cooling during the cure process of composite materials inducing severe residual stresses ([Guemes, 1994]; [Ogi and al., 1999]). Contrarily to the mechanical solicitation previously studied, the thermal expansion does not "break" the in-plane isotropy, thus the shear stresses and strains are null and the mechanical states independent of the orientation angle Θ of the reinforcing strip. One would notice that this result is also valid for any solicitation respecting the in-plane symmetry.

The local stresses inside the in-plane isotropic material are summed up in the Table 8 below. One can observe a marked gap between the σ_{xx} stresses in the two constituents: the matrix is subjected to traction, although the reinforcing strips are constricted; besides, this compression state implies a risk of micro-buckling at the surface of the material.

Table 8: Local stress states into the in-plane isotropic material

	STRESSES (MPA)		
	σ_{xx}	σ_{yy}	σ_{zz}
Effective material	0.0	0.0	0.0
Extra-reinforcement matrix	42.6	42.5	0.4
Reinforcing strips	-48.1	44.1	0.1

Inside a reinforcing strip, one can observe a compression of the fibers in the x-direction, while the resin is subjected to traction. In the normal direction z, one can also notice the emergence of complementary stresses in the fibers and the matrix, due to the gap on properties between these two constituents.

Table 9: Local stress states into the reinforcing strip

	STRESSES (MPA)		
	σ_{xx}	σ_{yy}	σ_{zz}
Effective reinforcement	-48.1	44.1	0.1
Intra-reinforcement matrix	57.79	55.51	25.39
Fibers	-109.9	37.5	-14.7

5 CONCLUSION AND PROSPECTIVES

A two-steps scale transition procedure based on Eshelby's inclusion has been introduced in order to describe the thermo-mechanical behaviour of an in-plane isotropic composite material, made of epoxy resin and carbon-epoxy reinforcing strips, exhibiting an in-plane distribution on the morphologies. The limits of the Kröner-Eshelby model for this kind of microstructures have been discussed, by comparing the results of the strain-based and stress-based formulations; each solution was discussed on the base of Hill's averages principles. A mixed formulation was then suggested and gave satisfying results in components of thermo-mechanical properties and mechanical states averages.

The previous framework and its results are applicable to other particles-reinforced materials such as nanocomposites, as the morphologies tested are close to those exhibited by carbon nanotubes. Thereby, the multimorphous model is an interesting alternative to the Krenchel model ([Krenchel, 1964 ; Thostenson and Chou, 2003]) which gives a simple estimate of the elastic properties of isotropic particles-reinforced materials.

The scale transition procedure was applied to two typical thermo-mechanical loadings. This enabled to calculate the local stresses in the material when experiencing mechanical and thermal loads. Theses loads and stresses are typical of those undergone by carbon-epoxy composite materials during the cooling of cure processes, and constitute an important issue for industrial applications. The complex evolution of residual stresses during cure process is mainly induced by the reticulation reaction of the organic matrix, with the associated chemical shrinkage, and the evolution of its properties. These stresses can be predicted within the framework developed above.
To conclude, this work has shown that the multi-morphous Kröner-Eshelby scale transition model is a powerful tool for the prediction of homogenized properties of composite materials and residual (or service) local stress states. However, for HEMs constituted by inclusions with very distinct morphologies, special attention must be paid to the uniqueness of the solution and the verification of Hill's averages principles.

6 REFERENCES

[Agbossou, 1997] Agbossou A, Pastor J, **Thermal stresses and thermal expansion coefficients of n-layered fiber-reinforced composites**, Composite Science and Technology **57**: 249-260, 1997.

[Baptiste, 2003] Baptiste D, **Non Linear Behavior Micromechanical Multi-scale Modelling of Discontinuous Reinforced Composites**, Mat. Sci. For., 426-432 : 3939-3944, 2003.

[Benveniste, 1987] Benveniste Y, **A new approach to the application of Mori-Tanaka's theory in composite materials,** Mechanics of Materials **6**: 147-157, 1987.

[Berryman and Berge, 1996] Berryman J, Berge P, **Critique of two explicit schemes for estimating elastic properties of multiphase composites**, Mechanics of Materials **22**: 149-164, 1996.

[Eshelby, 1957] Eshelby J D, **The Determination of the Elastic Field of an Ellipsoidal Inclusion, and Related Problems**, Proceedings of the Royal Society London, **A241**: 376–396, 1957.

[Guemes, 1994] J.A. Guemes, **Curing Residual Stresses and Failure Analysis in Composite Cylinders,** Journal of Reinforced Plastics and Composites, **13**: 408-419, 1994.

[Hill, 1967] Hill R., **The essential structure of constitutive laws for metals composites and polycrystals**, Journal of the Mechanics and Physics of Solids, **15**: 79-95, 1967.

Lacoste, E., **Fréour, S.,** Jacquemin, F. (2010). On the validity of the Kröner-Eshelby scale transition model for inclusions with various morphologies, *Mechanics of Materials*, **42**(2), 218-226.

[Kröner, 1958] Kröner E., **Berechnung der elastischen Konstanten des Vielkristalls aus des Konstanten des Einkristalls**, Zeitschrift für Physik, **151**: 504-508, 1958.

[Kocks and al., 1998] Kocks UF, Tomé CN, Wenk HR, **Texture and anisotropy**, Cambridge University Press, 1998.

[François, 1991] François M, **Détermination des contraintes résiduelles sur des fils d'acier eutectoïde de faible diamètre par diffraction des rayons X**, Doctoral Thesis, ENSAM Paris, 1991.

[Fréour, 2003] Fréour S, **« Application des modèles de transition d'échelle à la détermination des contraintes internes par diffraction des rayons X, cas des matériaux biphasés »**, Doctoral thesis, University of Nantes, 2003.

[Fréour and al., 2005] Fréour S, Jacquemin F, Guillén R, **On an analytical self-consistent model for internal stress prediction in fiber-reinforced composites submitted to hygroelastic load**, Journal of Reinforced Plastics and Composites, **24**: 1365-1377, 2005.

[Fréour and al., 2006] Fréour S, Jacquemin F, Guillén R, **Extension of Mori-Tanaka approach to hygroelastic loading of fiber-reinforced Composites – Comparison with Eshelby-Kröner self-consistent model**, Journal of Reinforced Plastics and Composites, **25**: 1039-1053, 2006.

[Jacquemin and al., 2005] Jacquemin F, Fréour S, Guillén R, **A hygroelastic self-consistent model for fiber-reinforced composites**, Journal of Reinforced Plastics and Composites, **24**: 485-502, 2005.

[Krenchel,1964] Krenchel H, **Fibre Reinforcements**, Akademisk Forlag, Copenhagen, 1964.

[Le Pen and Baptiste, 2002] Le Pen E, Baptiste D, **Multi-scale fatigue behaviour modelling of Al/Al_2O_3 short fibre composites by a micro-macro approach**, International Journal of Fatigue, **24**: 205-214, 2002.

[Ogi and al., 1999] K Ogi, HS Kim, T Maruyama, Y Takao, **The infuence of hygrothermal conditions on the damage processes in quasi-isotropic carbon/epoxy laminates**, Composites Science and Technology, **59**: 2375-2382, 1999.

[Roe, 1965] Roe R J, **Titre**, J. Appl. Phys., **36**: 2024, 1965.

[Thostenson&Chou,2003] Thostenson ET, Chou TW, **Titre,** J. Phys. D: Appl. Phys., **36**: 573, 2003.

Lacoste, E., **Fréour, S.,** Jacquemin, F. (2010). On the validity of the Kröner-Eshelby scale transition model for inclusions with various morphologies, *Mechanics of Materials*, **42**(2), 218-226.

[Treacy and al., 1996] Treacy, M.M.J., Ebbesen, T.W. et Gibson, T.M., **Exceptionally high Young's modulus observed for individual carbon nanotubes**, Nature, **381**: 678-680, 1996.

[Vook and Witt, 1968] F. Witt and R.W. Vook, **Titre**, J. Appl. Phys., **39**: 2773-2776, 1968.

[Welzel and Freour, 2007] U. Welzel, S. Fréour, **Generalisation of the Vook-Witt and inverse Vook-Witt elastic grain interaction models to general loading states,** Philosophical Magazine, 87: 3921-3943, 2007.